The Caspase-3 Precursor Has a Cytosolic and Mitochondrial Distribution: Implications for Apoptotic Signaling

Marie Mancini,* Donald W. Nicholson,¶ Sophie Roy,¶ Nancy A. Thornberry, Erin P. Peterson,** Livia A. Casciola-Rosen,‡§ and Antony Rosen*§‖**

*Department of Medicine, ‡Department of Dermatology, §Department of Cell Biology and Anatomy, ‖Department of Pathology, Johns Hopkins University School of Medicine, Baltimore, Maryland 21205; ¶Department of Biochemistry and Molecular Biology, Merck Frosst Center for Therapeutic Research, Pointe Claire-Dorval, Quebec, H9R 4P8, Canada; and **Department of Biochemistry, Merck Research Laboratories, Rahway, New Jersey 07065

Abstract. Caspase-3–mediated proteolysis is a critical element of the apoptotic process. Recent studies have demonstrated a central role for mitochondrial proteins (e.g., Bcl-2 and cytochrome *c*) in the activation of caspase-3, by a process that involves interaction of several protein molecules. Using antibodies that specifically recognize the precursor form of caspase-3, we demonstrate that the caspase-3 proenzyme has a mitochondrial and cytosolic distribution in nonapoptotic cells. The mitochondrial caspase-3 precursor is contained in the intermembrane space. Delivery of a variety of apoptotic stimuli is accompanied by loss of mitochondrial caspase-3 precursor staining and appearance of caspase-3 proteolytic activity. We propose that the mitochondrial subpopulation of caspase-3 precursor molecules is coupled to a distinct subset of apoptotic signaling pathways that are Bcl-2 sensitive and that are transduced through multiple mitochondrion-specific protein interactions.

Apoptosis is a controlled form of cell suicide that can be triggered by a variety of internal or external signals (for reviews see Thompson, 1995; White, 1996; Jacobson et al., 1997). Recent studies have demonstrated that specific protease activation is a critical element of the apoptotic process. In all systems described to date, the implicated proteases are members of a novel cysteine protease family which share an absolute requirement for aspartic acid in the P_1 position of proteolytic substrates (Martin and Green, 1995; Chinnaiyan and Dixit, 1996; Nicholson and Thornberry, 1997; Salvesen and Dixit, 1997). The 12 described members of the mammalian family of these proteases, which are all present as inactive precursors in resting cells, have been termed caspases (for **c**ysteinyl **asp**artate-specific protein**ase** [Alnemri et al., 1996]). During apoptosis, these precursors are cleaved at Asp-X sites, generating a large and small subunit, which together constitute the active protease. Numerous observations, including identification of the individual substrate specificities of the caspases, suggest that this protease family forms a multitiered proteolytic system that collectively responds to apoptotic stimuli (activator caspases) and manifests the apoptotic phenotype (effector caspases) (Liu et al., 1996; Orth et al., 1996; Muzio et al., 1997; Thornberry et al., 1997).

Activation of effector caspases, such as caspase-3, is the common event initiated by the multiple different stimuli that induce apoptosis. Signals are transduced by at least two pathways, which are differentially sensitive to Bcl-2: (*a*) The signals originating from the tumor necrosis factor receptor family (which are transduced through caspase-activating adaptor proteins such as FADD/MORT1 [Boldin et al., 1995; Chinnaiyan et al., 1995]), are largely Bcl-2 insensitive (for examples see Strasser et al., 1995; Chinnaiyan et al., 1996*b*; Erhardt and Cooper, 1996). These signals activate upstream caspases (e.g., caspases-6, -8, and -9), which catalyze the direct activation of pro-caspase-3 (Boldin et al., 1996; Liu et al., 1996; Muzio et al., 1996, 1997; Orth et al., 1996). Similar direct activation of the effector caspase pathway is accomplished by granzyme B (Darmon et al., 1995; Chinnaiyan et al., 1996*a*; Duan et al., 1996; Gu et al., 1996; Martin et al., 1996; Quan et al., 1996; Shi et al., 1996). (*b*) Signals originating from numerous other stimuli, including UVB irradiation, staurosporine treatment, growth factor deprivation, and p53 upregulation, are potently inhibited by Bcl-2 (Reed, 1994; Yin et al., 1994; Vaux and Strasser, 1996). The mechanism of activation of effector caspases in the Bcl-2–sensitive pathway has been elusive (Reed, 1997*b*), but recent evidence has underscored

Address all correspondence to Antony Rosen, Johns Hopkins University School of Medicine, 720 Rutland Ave., Room 1055, Baltimore, MD 21205. Tel.: (410) 955-0139. Fax: (410) 955-0964. E-mail: arosen@welchlink.welch.jhu.edu

the potential role of mitochondria and novel adaptor molecules in this pathway.

Significant data that strongly indicate a role for mitochondria in the initiation of apoptosis has now accumulated (for recent reviews see Henkart and Grinstein, 1996; Kroemer et al., 1997; Reed, 1997*a*,*b*; Vaux, 1997). Reconstitution experiments in a cell-free system using extracts of *Xenopus laevis* oocytes initially demonstrated that only cytoplasmic fractions enriched in mitochondria are able to induce nuclear apoptosis events (Newmeyer et al., 1994). In several cell types, changes in mitochondrial transmembrane potential consistent with permeability transition occur before the onset of nuclear apoptosis (Deckwerth and Johnson, 1993; Vayssiere et al., 1994; Castedo et al., 1995; Cossarizza et al., 1995; Macho et al., 1995; Petit et al., 1995; Zamzami et al., 1995*a*,*b*). In isolated mitochondria, agents that induce mitochondrial permeability transition release a novel "apoptosis-inducing factor" (AIF)[1] that is capable of initiating features of nuclear apoptosis in a cell-free system (Susin et al., 1996; Zamzami et al., 1996). During apoptosis, cytochrome *c*, which is normally located in the mitochondrial intermembrane space, is released. Together with other cytosolic factors, cytochrome *c* can trigger the activation of caspase-3 in a cell-free system (Liu et al., 1996; Kluck et al., 1997; Yang et al., 1997; Zou et al., 1997). Recent studies have suggested several mechanisms that may be responsible for cytochrome *c* release from mitochondria during apoptosis: (*a*) physical disruption of the outer mitochondrial membrane early in apoptosis occurring as a result of inner mitochondrial membrane hyperpolarization and matrix swelling, before permeability transition (Vander Heiden et al., 1997); (*b*) outer mitochondrial membrane rupture occurring as a secondary consequence of mitochondrial permeability transition (Susin et al., 1997). In all cases, changes in mitochondrial potential, volume homeostasis, and cytochrome *c* or AIF release are prevented by overexpression of Bcl-2 and similar family members (Zamzami et al., 1995*a*, 1996; Kluck et al., 1997; Vander Heiden et al., 1997; Yang et al., 1997).

While the release of cytochrome *c* from mitochondria is able to initiate activation of caspase-3 in cytosolic extracts in vitro, there is substantial evidence that the interaction of multiple proteins is essential for this to occur (Liu et al., 1996; Zou et al., 1997). Apaf-1, which shares homology with Ced-4, binds to cytochrome *c* and is required to initiate caspase-3 processing; caspase-9 is another integral component of the complex that initiates the processing of caspase-3 (Li et al., 1997; Zou et al., 1997). The subcellular site at which such multiprotein complexes might form during the initiation of Bcl-2–sensitive apoptosis has not yet been determined, but several observations highlight the mitochondrial outer membrane as a potential candidate. These include the observations that (*a*) Bcl-2 is enriched in the outer mitochondrial membrane (Krajewski et al., 1993); (*b*) CED-4 has the capacity to bind to both CED-9 and -3 (Chinnaiyan et al., 1997; Wu et al., 1997); and (*c*) coexpression of CED-9 alters the subcellular distribution of CED-4 from cytosol to a membrane fraction enriched in mitochondria (Wu et al., 1997).

To determine the subcellular distribution of the caspase-3 precursor, we generated antibodies that exclusively recognize the precursor form of caspase-3 and used these to study the distribution of caspase-3 in several different cell types before and during apoptosis. These studies show that in addition to its diffuse cytoplasmic location, the caspase-3 precursor also has a mitochondrial distribution. In morphologically apoptotic cells, mitochondrial staining of the caspase-3 precursor is absent. The mitochondrial enrichment of a central apoptotic effector molecule, with several molecules that regulate its activation, and the loss of this mitochondrial caspase-3 precursor pool during apoptosis suggest a mechanism whereby the apoptotic stimulus emanating from mitochondria is efficiently transduced.

Materials and Methods

Antibodies Recognizing the Precursor Form of Caspase-3

Generation of Antibody R280. The large subunit of caspase-3 was engineered as a MetSer29-Asp175 construct, expressed from an IPTG-inducible vector (pET11d; Novagen, Inc., Madison, WI) in *Escherichia coli* BL21(DE3)pLysS cells (Novagen, Inc.) and recovered by purification of inclusion bodies. The resulting recombinant protein (>98% pure as judged by SDS-PAGE) was denatured and resuspended in 6 M guanidine HCl, 25 mM Tris-HCl, pH 7.4, and used directly to immunize rabbits. Antibody MF393 was generated similarly and had identical characteristics (data not shown).

Characterization of Antibodies. (*a*) Immunoblotting. Recombinant caspase large subunits (caspases 1–10, excluding caspase 6, and Ced-3) were generated by expression in bacteria as described previously (Rotonda et al., 1996). 10 ng of each purified caspase large subunit was immunoblotted with antiserum R280. The antibody recognized the large subunit of caspase-3 exclusively (Fig. 1 *a*). (*b*) Immunoprecipitation. Recombinant caspase-3 was biotinylated by incubation with 10 nM of the irreversible inhibitor biotin-DEVD-acyloxymethylketone (L772,094) in buffer containing 50 mM Hepes pH 7.0, 2 mM EDTA, 0.1% (wt/vol) 3-([3-cholamidopropyl]-dimethyllammonio)-1-propanesulfonate (CHAPS), 10% (wt/vol) sucrose, and 5 mM DTT for 30 min at 37°C. Caspase-3 was then denatured by incubating either in 4 M guanidine-HCl/16.6 mM Tris-HCl, pH 7.4, at room temperature for 15 min, or in 0.7% (wt/vol) SDS in 67 mM Tris-HCl at 95°C for 5 min. 0.1-pmol amounts of the biotinylated native and denatured forms of caspase-3 were immunoprecipitated with R280 antiserum essentially as described (Taylor et al., 1995) (Fig. 1 *b*). Samples were visualized by immunoblotting with peroxidase-labeled streptavidin (Amersham Corp., Arlington Heights, IL) and enhanced chemiluminescence (ECL) (Amersham Corp.). R280 antiserum immunoprecipitated only the mature caspase-3 that had been denatured by boiling in SDS (Fig. 1 *b*). These results demonstrate that the R280 antiserum does not recognize the folded heterodimeric protease (although it can immunoprecipitate the precursor form of caspase-3 generated by coupled in vitro transcription/translation [data not shown]). (*c*) Competition Experiments. When decreasing amounts of antibody were used to immunoprecipitate a mixture of the precursor and mature forms of caspase-3 (generated by partially processing [^{35}S]methionine-labeled caspase-3 precursor with granzyme B), R280 exclusively immunoprecipitated the precursor form of caspase-3 (data not shown).

Affinity Purification of Antibodies. Purified p17 subunit of caspase-3 was spotted onto Immobilon (Millipore Corp., Bedford, MA) and used to affinity purify antibodies to caspase-3 from R280 antiserum as described (Olmsted, 1981). The amount of antibody was quantitated by comparing immunoblots of the affinity-purified antibody to dilutions of rabbit IgG standards. When these affinity-purified antibodies were used to immunoblot lysates of human umbilical vein endothelial cells (HUVECs) (Fig. 1 *c*), HeLa cells (data not shown), or keratinocytes (data not shown), they

1. *Abbreviations used in this paper*: AIF, apoptosis-inducing factor; CHAPS, 3-([3-cholamidopropyl]-dimethyllammonio)-1-propanesulfonate; DAPI, 4′,6-diamidino-2-phenylindole; DFF, DNA fragmentation factor; ECL, enhanced chemiluminescence; HUVEC, human umbilical vein endothelial cells; KGM, keratinocyte growth medium; KRB, Krebs' Ringers buffer; PARP, poly (ADP-ribose) polymerase.

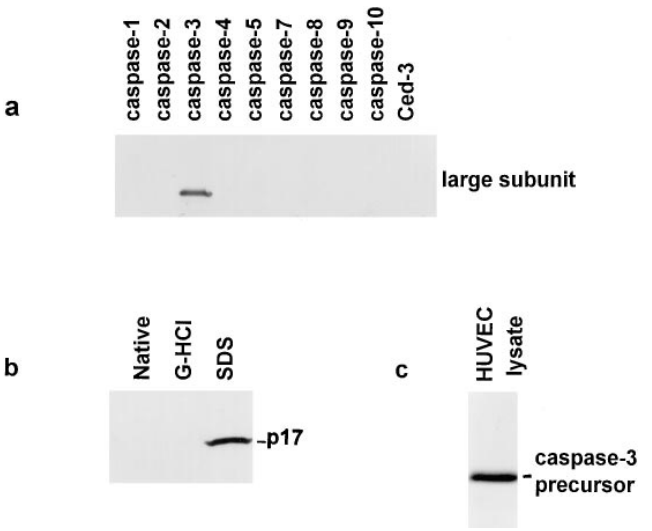

Figure 1. Characterization of anti–caspase-3 antiserum (R280). (*a*) 10-ng amounts of the purified large subunits (caspases 1–10, excluding caspase-6) and Ced-3 were immunoblotted with R280 antiserum. (*b*) Biotinylated recombinant mature caspase-3 was denatured by treatment with guanidium-HCl or SDS, as described in the Materials and Methods section. Native and denatured biotinylated caspase-3 were subsequently immunoprecipitated using R280, and the p17 subunit was detected by immunoblotting. (*c*) 46 μg of HUVEC lysate was immunoblotted with affinity-purified R280 antiserum. Similar results were obtained when keratinocyte lysates were immunoblotted with affinity-purified R280 antiserum (data not shown).

recognized only the caspase-3 precursor. A very minor band (<2% of the caspase-3 precursor intensity) of 120 kD was variably seen.

Cell Culture and Induction of Apoptosis

Human keratinocytes were obtained from neonatal foreskins and cultured in keratinocyte growth medium (KGM) (Clonetics Corp., San Diego, CA) as described (Casciola-Rosen et al., 1994*a*). Confluent secondary monolayers were used for experiments. HUVECs were obtained from Clonetics Corp., grown in endothelial cell growth medium (Clonetics Corp.), and used at the third or fourth passage. HeLa and WIF-B cells were cultured as described (Ihrke et al., 1993; Casciola-Rosen et al., 1994*b*). Apoptosis was induced by irradiation with UVB (Casciola-Rosen et al., 1994*a*), C2-ceramide (Haimowitz-Friedman et al., 1994), or staurosporine (Jacobson et al., 1996).

Visualization of Mitochondria and the Caspase-3 Precursor by Immunofluorescence Microscopy

Immunofluorescence was performed on cells that had been grown on No. 1 glass coverslips.

Labeling of Caspase-3. Cells were fixed with 4% paraformaldehyde for 5 min at 4°C before being permeabilized with acetone (30 s at 4°C). To visualize the precursor form of caspase-3, cells were incubated for 30 min on ice with 10 μg/ml affinity-purified anti–caspase-3 antibody (R280) and then washed in PBS before incubating with fluorescein-conjugated goat anti–rabbit IgG (Jackson ImmunoResearch Laboratories, Inc., West Grove, PA) for 20 min at room temperature.

Labeling of Mitochondria. Mitochondria were labeled in intact cells with MitoTracker™ CMXRos-H_2 (Molecular Probes, Inc., Eugene, OR) according to the manufacturer's directions. Briefly, MitoTracker was diluted to a final concentration of 1 μM in serum-free medium (KGM for keratinocytes and DME for HUVECs). Coverslips containing viable keratinocytes and HUVECs were incubated in the appropriate MitoTracker-containing medium for 30–45 min in a 5% CO_2 humidified incubator. The cells were then fixed and permeabilized and either mounted immediately (for single-labeled mitochondria) or were double-labeled with anti–caspase-3 antibody R280 as described above. When specified, nuclei were visualized by labeling with 4′,6-diamidino-2-phenylindole (DAPI) (Molecular Probes, Inc.). In all cases, coverslips were mounted on glass slides with PermaFluor (Lipshaw, Pittsburgh, PA), and confocal microscopy was performed on a scanning confocal microscope system (model LSM 410; Carl Zeiss, Inc., Thornwood, NY).

Immunoelectron Microscopy

Immuno-EM was performed essentially as described (Berryman et al., 1992). Briefly, WIF-B cells (Ihrke et al., 1993) were fixed at room temperature for 10 min (3% paraformaldehyde, 0.05% glutaraldehyde in Hank's salt solution) and scraped, and the cell pellet was fixed for an additional 45 min in this fixative. Cell pellets were washed with 3.5% sucrose in 0.1 M phosphate buffer, pH 7.4 (SPB), and postfixed with 0.25% tannic acid in SPB for 60 min at 0°C before quenching free aldehydes for 60 min with 50 mM ammonium chloride in SPB. After washing in sucrose-maleate buffer, pH 6.5, containing 4% sucrose, cells were stained en bloc with 2% uranyl acetate in sucrose-maleate buffer, pH 6.0, dehydrated, and embedded in LR gold resin at −20°C. Silver-gold sections were mounted on formvar-coated 200-mesh nickel grids, blocked in 1% BSA/TBST (10 mM Tris, pH 7.2, 500 mM NaCl, and 0.05% Tween 20), and stained for 2.5 h with affinity-purified R280 antibodies (15 μg/ml). After rinsing, grids were stained for 60 min with 12-nm colloidal gold-labeled donkey anti–rabbit IgG (Jackson ImmunoResearch Laboratories, Inc.; OD_{520} = 0.05 [1:40 dilution]) followed by 2% aqueous osmium tetroxide (15 min) and then counterstained for 3 min with Reynold's lead citrate. Sections were viewed and photographed in an electron microscope (TEM type 1A; Carl Zeizz, Inc.), and prints were made to a final enlargement of 21,000 magnification. For quantitation, the area of mitochondria and extramitochondrial structures was measured, and the number of gold particles/cm^2 associated with mitochondria or other organelles was calculated (>200 gold particles in 10 separate prints were quantitated).

Western Blot Analysis of Caspase-3 in Mitochondria Isolated from Human Liver

Mitochondria were isolated from human liver recovered at autopsy of a 17-yr-old male (cause of death: accidental) or rat liver as previously described (Nicholson and McMurray, 1984). All steps were performed at 4°C. The tissue was rinsed in SME buffer (0.25 M sucrose, 10 mM MOPS, 2 mM EDTA, pH 7.4), rid of blood vessels, and dispersed in SME buffer. The suspension was centrifuged twice at 480 *g* to sediment out nuclei and large cellular debris, and the mitochondria were recovered by centrifugation at 4,300 *g* for 10 min followed by a 2-min centrifugation at 10,000 *g*. After washing the mitochondrial pellet four times in SME buffer to minimize microsomal contamination, the mitochondria were resuspended in SME buffer to a protein concentration of 16 mg/ml and stored at −80°C.

To perform the experiments shown in Fig. 3, mitochondria (200 μg) were diluted in SME buffer with or without NP-40 (final concentration 1%). After a 1-h incubation at 37°C in the presence or absence of 0.2 μg granzyme B, the mitochondrial suspension was analyzed by SDS-PAGE and immunoblotted with the R280 anti–caspase-3 antibody essentially as described (Scoggan et al., 1996) except that the primary antibody was used at a dilution of 1:5,000. Identical results were obtained when mitochondria were disrupted by repeated freeze-thaw (data not shown). Progressive digitonin extraction and enzyme assays to measure adenylate kinase and fumarase were performed exactly as described on freshly isolated mitochondria (Nicholson et al., 1987).

Subcellular Fractionation of HeLa Cells

Mitochondrial and cytosolic fractions were obtained by differential centrifugation of HeLa cell homogenates as described (Vander Heiden et al., 1997). Briefly, cells were washed twice with PBS, scraped, pelleted, and resuspended in 2.5 ml of ice-cold buffer A (250 mM sucrose, 20 mM Hepes, pH 7.4, 10 mM KCl, 1.5 mM $MgCl_2$, 1 mM EGTA, 1 mM EDTA, 1 mM DTT, and the protease inhibitors PMSF, leupeptin, chymostatin, pepstatin, and antipain). Cells were homogenized with a Balch/Rothman homogenizer (Balch and Rothman, 1985), with ball bearings that allowed calculated clearances of 0.0019 in or 0.0011 in. A postnuclear supernatant was prepared and centrifuged at 10,000 *g* for 25 min to obtain a pellet highly enriched in mitochondria. The pellet was resuspended in a volume of buffer A equal to that of the postmitochondrial supernatant. The postmitochondrial supernatant was further centrifuged at 100,000 *g* to obtain cytosol. Equivalent volume amounts of mitochondrial and cytosolic frac-

tions were electrophoresed on 13.5% SDS–polyacrylamide gels, transferred to polyvinyl difluoride, and immunoblotted with R280 (1:5,000) or monoclonal antibodies to human cytochrome *c* (mAb 7H8.2C12 at 1.5 μg/ml; Pharmingen, San Diego, CA) and cytochrome oxidase (subunit IV) (mAb 20E8-C12 at 0.1 μg/ml; Molecular Probes, Eugene, OR). Relative distributions of proteins in the two fractions were assessed by densitometry as described below. While >95% of cytochrome *c* was associated with the mitochondrial fraction in cells homogenized with a ball bearing clearance of 0.0019 in, >95% of cytochrome *c* was found in the cytosol when cells were homogenized with a ball bearing clearance of 0.0011 in (Fig. 3 *c* and data not shown; seven separate experiments). In contrast, >95% of cytochrome oxidase was located in the mitochondrial fraction regardless of the ball bearing clearance (Fig. 3 *c* and data not shown).

Purification of Human Granzyme B

Granzyme B was purified from granules isolated from cultured human natural killer leukemia YT cells essentially as described (Hanna et al., 1993; Quan et al., 1995). The granule contents were extracted with NaCl (the calcium was omitted), diluted, and then loaded onto a Mono-S cation-exchange column (0.5 × 0.5 cm; Pharmacia Biotech, Inc., Piscataway, NJ) that had been pre-equilibrated in 50 mM MES, pH 6.1, 25 mM NaCl. After washing with 12 vol of equilibration buffer, proteins were eluted with a linear gradient up to 1 M NaCl (in 50 mM MES, pH 6.1) over 40 column volumes. Granzyme B eluted at ~0.6 M NaCl and was homogenous as judged by SDS-PAGE.

Cleavage Assays to Measure Endogenous Caspase-3 Activity

Generation of Cell Lysates. Control or apoptotic keratinocytes (incubated for the indicated times after UVB irradiation) were washed in Krebs Ringers buffer (KRB) containing 20 mM Hepes/NaOH, pH 7.4, 10 mM dextrose, 127 mM NaCl, 5.5 mM KCl, 1 mM $CaCl_2$, and 2 mM $MgSO_4$, and then harvested by scraping into KRB, followed by centrifugation at 300 *g*. The harvested cells were lysed in buffer containing 10 mM Hepes/KOH, pH 7.4, 2 mM EDTA, 1 mM DTT, 1% NP-40 (vol/vol), and the protease inhibitors PMSF, antipain, leupeptin, and pepstatin A to obtain whole cell lysates (protein concentration = 2.5 mg/ml). Aliquots of lysates were taken for protein assays, and DTT was then added to samples to obtain a final concentration of 5 mM DTT.

In Vitro Cleavage of Endogenous Poly (ADP-Ribose) Polymerase. Whole cell lysates were incubated for 0 or 2 h at 37°C, as indicated in Fig. 7, before the addition of SDS electrophoresis sample buffer. Samples were electrophoresed on 10% SDS–polyacrylamide gels containing 0.087% bisacrylamide, and the proteins were transferred to nitrocellulose. Endogenous poly (ADP-ribose) polymerase (PARP) was detected by immunoblotting with a patient serum monospecific for PARP as described (Casciola-Rosen et al., 1995). The densities of bands on autoradiograms were determined on a PDI Discovery densitometry system (Protein Databases, Inc., Huntington Station, NY) with Quantity One software (Protein Databases, Inc.).

Cleavage of Ac-DEVD-Aminomethylcoumarin by Cell Lysates. To measure Ac-DEVD-aminomethylcoumarin (Ac-DEVD-AMC) cleavage activity, lysates were added to reaction mixtures containing 10 or 100 μM Ac-DEVD-AMC, 100 mM Hepes, 10% sucrose, 0.1% CHAPS, 0.1 mM EDTA, and 1 mM DTT, pH 7.5, in a total volume of 100 μl. Production of AMC was monitored continuously at ambient temperature in an SLT Fluostar 96-well plate reader (Tecan U.S. Inc., Research Triangle Park, N.C.) using an excitation wavelength of 380 nm and an emission wavelength of 460 nm. To confirm that the observed activity was due to caspase-3 or a closely related homologue, each sample was tested for inhibition by *N*-ethylmaleimide, Ac-DEVD-CHO (K_i caspase-3 = 0.35 nM), and Ac-YVAD-CHO (K_i caspase-3 = 10,000 nM). Activities that were inhibited by *N*-ethylmaleimide (5 mM) and Ac-DEVD-CHO (500 nM) but not by Ac-YVAD-CHO (500 nM) were attributed to caspase-3 or a closely related homologue. Activity is expressed in U/mg, where a unit is defined as the amount of enzyme required to produce 1 pmol of AMC per min using 100 μM Ac-DEVD-AMC.

Results

The Caspase-3 Precursor Has a Cytosolic and Mitochondrial Distribution

The subcellular location of the caspase-3 precursor in human foreskin keratinocytes was first determined with confocal fluorescence microscopy (Fig. 2). Using affinity-puri-

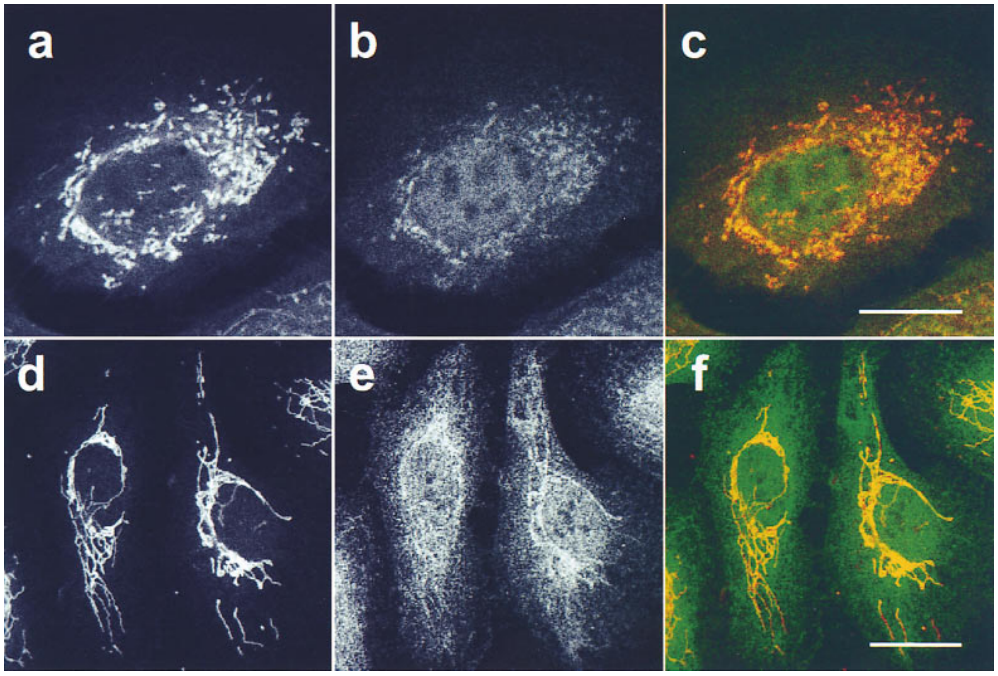

Figure 2. Caspase-3 is localized in the cytosol and mitochondria of keratinocytes and HUVECs. Keratinocytes (*a–c*) and HUVECs (*d–f*) were labeled with MitoTracker, fixed, permeabilized, and stained with affinity-purified polyclonal rabbit anti–caspase-3 precursor antibody (R280) as described in Materials and Methods. The stained cells were examined by confocal immunofluorescence microscopy. Caspase-3 antibodies were visualized with fluorescein-conjugated goat anti–rabbit IgG and assigned the color green (*b* and *e*), whereas mitochondria labeled with MitoTracker were assigned the color red (*a* and *d*). When red and green images were merged, overlapping red and green pixels appeared orange/yellow (*c* and *f*). The experiments were repeated on 11 (*a–c*) or 4 (*d–f*) separate occasions with identical results. Bar, 10 μm.

fied polyclonal antibody R280, which exclusively recognizes the caspase-3 precursor (see Materials and Methods), a diffuse cytosolic staining pattern with a superimposed punctate perinuclear component was obtained; low levels of diffuse nuclear staining were also observed (Fig. 2 *b*). The punctate component appeared similar to that seen for mitochondria, prompting us to double-stain keratinocytes with a mitochondrion-selective vital dye (MitoTracker) and R280. These studies confirmed that mitochondria were distributed in a punctate, perinuclear pattern in keratinocytes (Fig. 2 *a*), and that the punctate fraction of caspase-3 colocalized with mitochondria (Fig 2 *c*; overlapping red and green pixels seen as yellow).

The specificity of the caspase-3 precursor staining was confirmed in the following ways: (*a*) Competition experiments were performed by preincubating affinity-purified anti–caspase-3 (R280) antibody with a 100-fold excess of its p17 cognate antigen before use in immunofluorescence. In cells stained with these preincubated antibodies, the punctate pattern (mitochondria) was abolished, and the diffuse cytoplasmic staining was greatly diminished (data not shown). Since nuclear staining was minimally affected, this most likely represents nonspecific binding (data not shown). In contrast, when the anti–caspase-3 antibody was similarly preincubated with the p20 subunit of caspase-1, the punctate staining and diffuse cytoplasmic staining were not affected (data not shown). (*b*) No staining was observed when keratinocytes were incubated with secondary antibody alone, nor when an affinity-purified anti–caspase-1 antibody was used (data not shown). (*c*) When cells were single-stained with anti–caspase-3 antibodies, an identical punctate staining pattern was seen, confirming that this pattern was directly due to antibody binding, rather than bleedthrough between channels in the double-stained samples (data not shown). (*d*) Perinuclear punctate and diffuse cytoplasmic staining patterns were observed when cells were fixed with 2% paraformaldehyde/0.5% glutaraldehyde; the level of cytoplasmic staining was increased and nuclear staining was decreased using this fixation technique (data not shown). (*e*) An identical staining pattern was observed when a different rabbit anti–caspase-3 precursor serum (antibody MF393; raised against the unfolded p17 subunit of caspase-3) was used to stain keratinocytes (data not shown). Taken together, these data show that the caspase-3 precursor has a cytosolic and mitochondrial distribution in keratinocytes.

To examine whether this distribution was unique to keratinocytes, similar immunofluorescence experiments were performed using several other cell types. In HUVECs, mitochondria stained with a filamentous pattern that extended through the cytoplasm to the cell periphery (Fig. 2 *d*). The caspase-3 precursor shared an identical filamentous pattern but was also present diffusely in the cytoplasm (Fig. 2 *e*). Double staining confirmed colocalization of caspase-3 precursor and mitochondria (Fig. 2 *f*; overlapping red and green pixels seen as yellow). A similar mitochondrial and cytosolic distribution of the caspase-3 precursor was also observed in several other cells, including primary human myoblasts and myotubules, primary differentiated human neuronal cell cultures, MDCK cells, HeLa cells, and WIF-B cells (data not shown).

To confirm biochemically that the caspase-3 precursor is

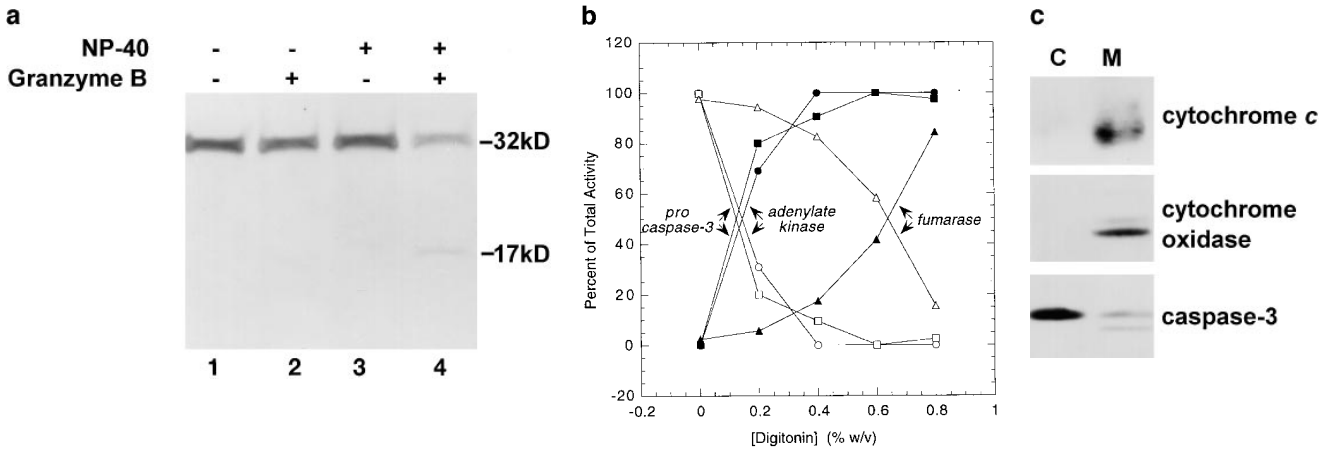

Figure 3. Biochemical analysis of mitochondrial caspase-3 precursor. (*a*) Caspase-3 precursor is detected by immunoblotting in human liver mitochondria. 200-μg aliquots of mitochondria, prepared from human liver as described in Materials and Methods, were incubated for 1 h at 37°C in the presence of the following: no additions (lane *1*), 0.2 μg granzyme B (lane *2*), 1% NP-40 (lane *3*), or 1% NP-40 and 0.2 μg granzyme B (lane *4*). Equal aliquots of these samples were electrophoresed and immunoblotted with the R280 anti–caspase-3 antibody. Note that the R280 antibody does not blot the 17-kD active enzyme well; the exposure shown in the figure was chosen to optimize visualization of the decreased 32-kD precursor caspase-3 (lane *4*). The results shown are representative of three separate experiments. (*b*) Mitochondrial pro-caspase-3 colocalizes with adenylate kinase in the intermembrane space. Freshly isolated rat liver mitochondria were sub-fractionated by progressive digitonin treatment as described in Materials and Methods. Marker enzyme activities for the intermembrane space (adenylate kinase; *circles*) and matrix (fumarase; *triangles*) were measured in the resulting supernatants (*solid symbols*) and pellets (*open symbols*). Pro-caspase-3 (*squares*) was detected in the same fractions by immunoblotting using the R280 antibody that cross-reacts with rat pro-caspase-3. Marker enzyme and pro-caspase-3 distributions in supernatants and pellets are expressed as a percentage of the total recovered. (*c*) Distribution of caspase-3 precursor in HeLa cells. HeLa cells were fractionated into cytosolic (*C*) and mitochondrial (*M*) fractions as described in Materials and Methods. Equivalent volume amounts of cytosolic and mitochondrial fractions were electrophoresed, and relative amounts of caspase-3 precursor, cytochrome *c*, and cytochrome oxidase (subunit IV) were determined by immunoblotting. Results are representative of two separate experiments.

localized in mitochondria, intact mitochondria were prepared and immunoblotted with R280 antibodies. The 32-kD caspase-3 precursor alone was detected in these samples (Fig. 3 *a*, lane *1*). To address whether caspase-3 was contained within these organelles or was associated with the outer surface, we incubated mitochondria in the presence of granzyme B, a cytolytic lymphocyte granule protease known to induce the processing and activation of caspase-3 (Darmon et al., 1995; Quan et al., 1996). In NP-40–permeabilized mitochondria (Fig. 3 *a*, lane *4*), but not in mitochondria incubated in the absence of detergent (Fig. 3 *a*, lane *2*), addition of granzyme B produced an 80% decrease in the amount of immunoblotted caspase-3 precursor, with concomitant appearance of the p17 subunit, as previously described (Martin et al., 1996; Quan et al., 1996). Similar results were obtained when repeated freeze-thawing was used to permeabilize mitochondria (data not shown). These biochemical data confirm the morphological finding that the caspase-3 precursor has a mitochondrial distribution and indicate that it is contained within the organelle.

To investigate the submitochondrial location of the caspase-3 precursor biochemically, purified mitochondria were treated with increasing concentrations of digitonin before recentrifugation. The relative amounts of the caspase-3 precursor, adenylate kinase (a mitochondrial intermembrane space marker enzyme), and fumarase (a mitochondrial matrix marker) were assayed in the resulting pellets and supernatants. The release of caspase-3 precursor from mitochondria at progressively higher digitonin concentrations coincided with adenylate kinase, with 50% of the total appearing in the supernatant at 0.15% (adenylate kinase) and 0.125% (caspase-3 precursor) digitonin (Fig. 3 *b*). In contrast, 50% fumarase release into the supernatant only occurred at 0.65% digitonin (Fig. 3 *b*).

Since intermembrane space contents frequently leak from mitochondria during subcellular fractionation procedures, establishing an accurate stoichiometry of distribution of caspase-3 precursor in mitochondrial versus post-mitochondrial fractions required a fractionation procedure that maintained the outer mitochondrial membrane integrity (see Materials and Methods). Cytochrome *c* and cytochrome oxidase (subunit IV) were used as markers of the intermembrane space and inner membrane, respectively. Under homogenization conditions where >95% of cytochrome *c* was retained in mitochondria, the amount of caspase-3 precursor in mitochondria was ~10% that found in cytosol (equal cell equivalents assayed; Fig. 3 *c*). In several separate experiments, caspase-3 immunoblotted as both the intact 32-kD form and a 29-kD form, most likely representing the protease without its prodomain (Fig. 3 *c*). In contrast, very low levels (<1%) of caspase-3 precursor were retained in mitochondria under conditions where >90% of cytochrome *c* was present in the cytosol (data not shown). Taken together, these data demonstrate that a significant proportion of the caspase-3 precursor is mitochondrial in distribution. Furthermore, since caspase-3 precursor is released from mitochondria at digitonin concentrations almost identical to those required to release adenylate kinase (Fig. 3 *b*) and retained in mitochondria only during homogenization conditions that maintain cytochrome *c* in the intermembrane space (Fig. 3 *c*), we conclude that caspase-3 is most likely located in the mitochondrial intermembrane space. These data are also consistent with the inaccessibility of the caspase-3 precursor to granzyme B in nonpermeabilized mitochondria (Fig. 3 *a*). It is also possible that the caspase-3 precursor is tightly associated with the outer surface of mitochondria.

To further confirm the ultrastructural localization of the mitochondrial caspase-3 precursor, ultrathin sections of WIF-B (Fig. 4) and HeLa cells (data not shown) were immunolabeled with affinity-purified R280 antibodies. Immunogold labeling was predominantly mitochondrial (63 ± 13%; $n = 8$ pictures, mean ± SD) and cytosolic (37 ± 12%; $n = 8$, mean ± SD); <5% of labeling was associated with other structures, including nucleus, endoplasmic reticulum, and plasma membrane (data not shown). The density of mitochondrial labeling (0.33 ± 0.09 gold particles/cm^2; $n = 246$ mitochondria, mean ± SD) was approximately sixfold higher than that observed in all areas outside mitochondria (0.05 ± 0.02 gold particles/cm^2). 30–50% of mitochondria were labeled with at least one gold particle; frequent examples of mitochondria labeled with multiple gold particles were found. It must be noted that significant extraction of cytosolic contents occurs during the fixation used to preserve optimal immunogenicity of the caspase-3 precursor for R280. It is likely that loss of cytosolic caspase-3 under these circumstances results in the different stoichiometries of caspase-3 distribution observed with biochemical and morphological methodologies. In all instances where mitochondrial labeling was observed, gold labeling was inside mitochondria, in close proximity to mitochondrial membranes. Particles were detected both immediately inside the outer membrane, most likely in the intermembrane space (Fig. 4, *a* and *c*) or well within the organelle, always near mitochondrial inner membrane cristae (Fig. 4, *a*, *b*, and *d*, and data not shown). These gold particles were found both alongside the membrane or within the cristal lumen (Fig. 4 *c*). Since the space within cristae is continuous with the intermembrane space, these data further support the confocal and biochemical data that localize the caspase-3 precursor to the mitochondrial intermembrane space.

Mitochondrial Staining of the Caspase-3 Precursor Is Absent in Morphologically Apoptotic Cells

Previous studies have described several novel features of mitochondria during apoptosis, including cytosolic leakage of cytochrome *c* (Liu et al., 1996; Kluck et al., 1997; Yang et al., 1997), and loss of mitochondrial transmembrane potential (for review see Kroemer et al., 1997). To determine the subcellular distribution of the caspase-3 precursor after induction of apoptosis, we performed immunofluorescence confocal microscopy on keratinocytes rendered apoptotic by irradiation with UVB. Nonirradiated cells showed the mitochondrial and cytosolic patterns of caspase-3 precursor staining described above (Fig. 5 *b*). In apoptotic cells, caspase-3 precursor staining was diminished, with no mitochondrial staining pattern visible (Fig. 5 *e*). In merged images, MitoTracker-stained mitochondria therefore appeared red (Fig. 5 *f*) rather than yellow (Fig. 5 *c*). A similar disappearance of mitochondrial caspase-3 precursor staining was observed in UVB-irradiated HUVECs and HeLa

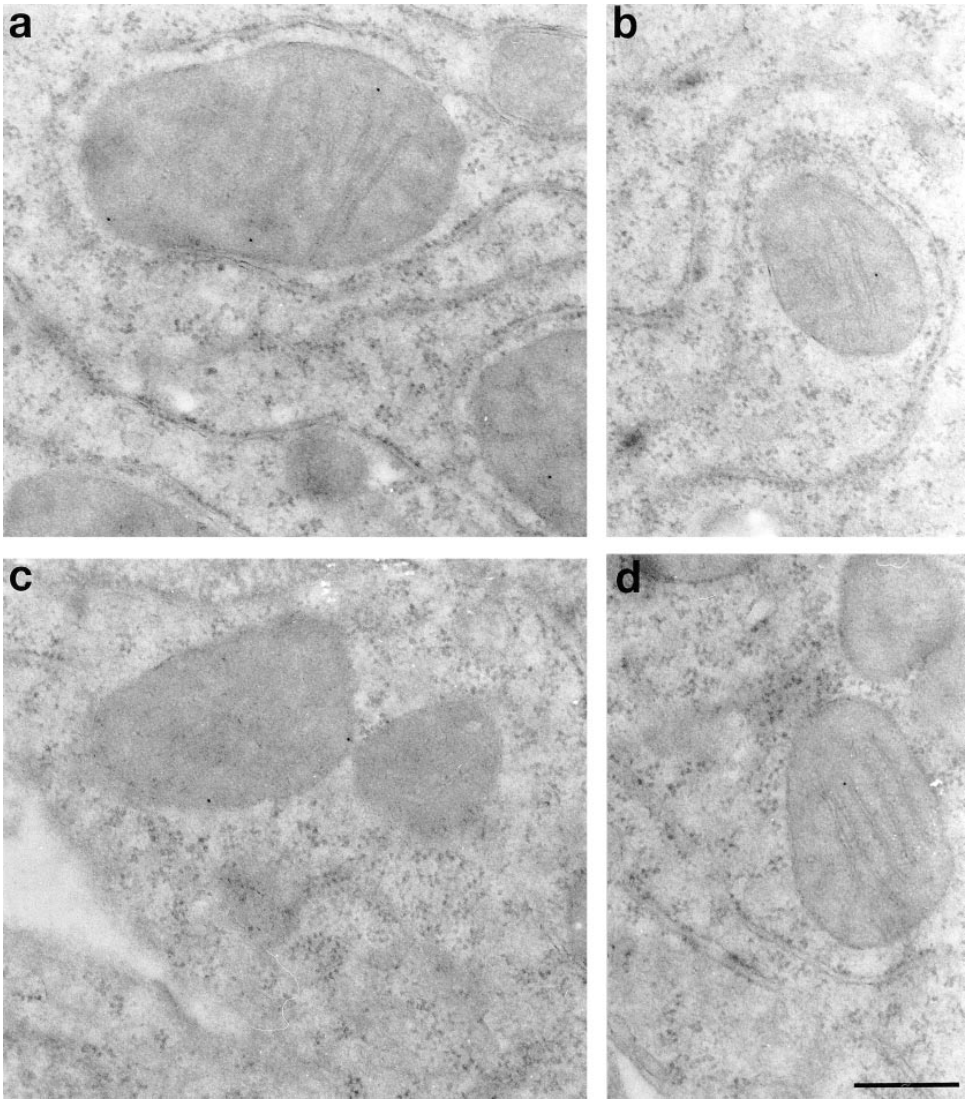

Figure 4. Immunolocalization of the caspase-3 precursor. Ultrathin sections of cultured WIF-B cells were labeled with affinity-purified R280 antibodies and 12-nm colloidal gold conjugated to donkey anti–rabbit IgG. *a–d* show caspase-3 precursor staining within mitochondria. Gold particles were localized to just inside the outer membrane (*a* and *c*), as well as to inner membrane cristae (*a*, *b*, and *d*). Omission of primary antibody resulted in the complete abolition of both cytosolic and mitochondrial staining (data not shown). Similar results were obtained in HeLa cells (data not shown). Bar, 300 nm.

cells, as well as in keratinocytes and HeLa cells in which apoptosis was induced with C2-ceramide (data not shown). Interestingly, no enrichment of caspase-3 precursor staining was observed in apoptotic surface blebs (Fig. 5 *e*, *arrowheads*), although we have detected the mature active enzyme in these structures (data not shown).

We also addressed the effects of staurosporine treatment on the mitochondrial staining of the caspase-3 precursor in keratinocytes (Fig. 6) and HeLa cells (data not shown). This agent does not induce the characteristic surface blebbing and cytosolic shrinkage of apoptosis but does induce classic nuclear condensation and fragmentation (detected by DAPI staining in Fig. 6 *a*), caspase-mediated substrate cleavage, and internucleosomal DNA degradation (Jacobson et al., 1996; and data not shown). Since apoptosis occurs asynchronously in cell populations, adjacent nonapoptotic and apoptotic cells can be visualized simultaneously. In cells with the condensed, fragmented nucleus characteristic of apoptotic cells (Fig. 6 *a*, *arrowheads*), mitochondrial caspase-3 staining was absent (Fig. 6 *b*, *arrowhead*). In this field, the adjacent cell with a nonapoptotic chromatin pattern (Fig. 6 *a*, *arrow*) had normal mitochondrial staining of the caspase-3 precursor (Fig. 6 *b*, *arrow*). Interestingly, unlike cells in which apoptosis was induced by UV irradiation, mitochondria in staurosporine-treated apoptotic cells that lacked caspase-3 staining also failed to label with MitoTracker, indicating a markedly reduced mitochondrial transmembrane potential, possibly due to permeability transition.

Appearance of Caspase-3 Activity in Apoptotic Cells

Since antibody R280 recognizes only the caspase-3 precursor, decreased R280 staining in apoptotic cells is consistent with activation of caspase-3. To address biochemically whether the caspase-3 activity was present in cell populations containing morphologically apoptotic cells that lacked mitochondrial staining with antibody R280, we measured cleavage of an exogenous peptide substrate (Ac-DEVD-AMC) in keratinocyte or HeLa cell lysates known to support the activity of caspase-3 (Nicholson et al., 1995; Casciola-Rosen et al., 1996). In nonirradiated cells, background levels of Ac-DEVD-AMC cleavage activity were observed (14 U/mg); these did not increase up to 4 h after irradiation of parallel cultures (Fig. 7 *a*). Consistent with the presence of numerous apoptotic cells at time points >6 h

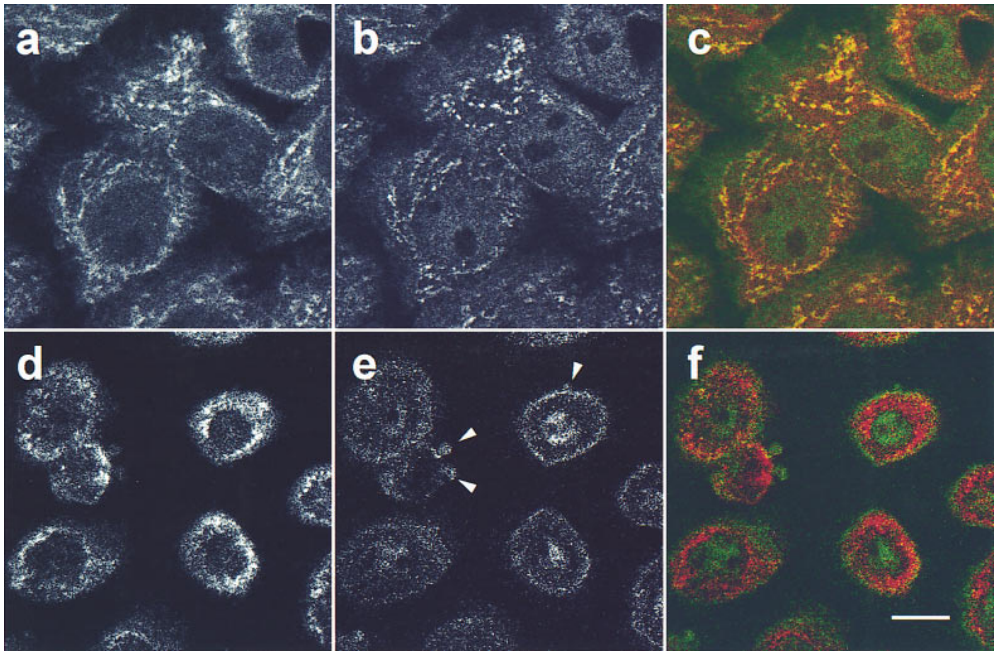

Figure 5. Lack of mitochondrial caspase-3 precursor staining in keratinocytes induced to become apoptotic by UVB irradiation. Control nonirradiated keratinocytes (*a–c*) or keratinocytes UVB-irradiated and subsequently incubated for 8 h (*d–f*) were labeled with MitoTracker and then fixed, permeabilized, and stained with R280. Mitochondrial staining was visualized in red (*a* and *d*), whereas pro-caspase-3 staining was visualized in green (*b* and *e*). When images were merged (*c* and *f*), overlapping red and green pixels appeared orange/yellow. Arrowheads denote apoptotic surface blebs. Experiments were repeated on 10 separate occasions with similar results. Bar, 10 μm.

after UVB irradiation, there was a marked increase in Ac-DEVD-AMC cleavage activity 8 h after irradiation (53 U/mg) (Fig. 7 *a*). The sensitivity of this activity to aldehyde inhibitors (Ac-DEVD-CHO but not Ac-YVAD-CHO) confirms that the activity is due to caspase-3 or a closely related homologue (data not shown). Similarly, cleavage of PARP, an endogenous macromolecular caspase-3 substrate, was only observed in cells incubated >6 h after UV irradiation (data not shown, and Fig. 7 *b*, lanes *1–6*), providing additional biochemical evidence for the coincident presence at times >6 h after UVB irradiation of caspase-3 activity, morphologic apoptosis, and loss of mitochondrial caspase-3 precursor staining.

Discussion

Cytoplasmic and Mitochondrial Distribution of the Caspase-3 Precursor in Nonapoptotic Cells

Activation of caspase-3 is a central event in the apoptotic process, upon which numerous different signaling pathways converge and through which multiple downstream substrates are cleaved. Recent data have strongly implicated the mitochondrion as a central integrating organelle in apoptotic signaling, which has the capacity to directly activate the execution pathways (see below). The studies reported here demonstrate that the caspase-3 precursor is present in both the cytosol and mitochondria in nonapoptotic cells. The existence of two spatially separate pools of the caspase-3 precursor predicts the existence of distinct activation pathways, regulated by different modulators of apoptosis. We propose that the mitochondrial caspase-3 precursor functions principally in Bcl-2–sensitive apoptotic pathways.

While it remains unclear how the caspase-3 precursor reaches its mitochondrial location, it is possible that it might either possess a cryptic targeting sequence (as does cytochrome *c*) or might interact with other molecules that target it to mitochondria. Identifying any interacting proteins and determining whether the mitochondrial and cy-

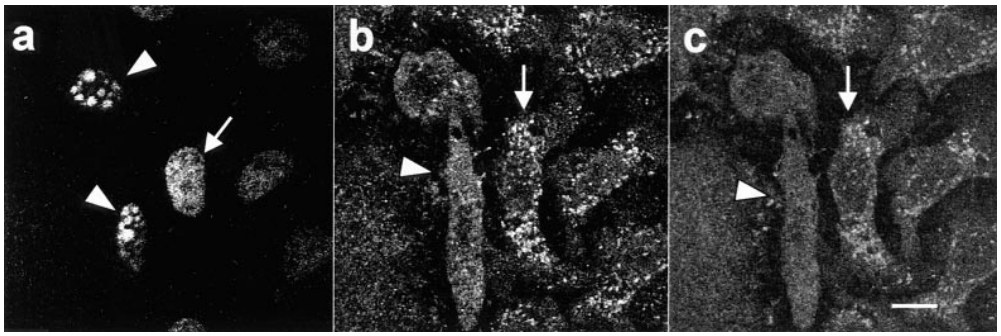

Figure 6. Lack of mitochondrial caspase-3 precursor staining and MitoTracker labeling in staurosporine-induced apoptosis. Keratinocytes were incubated with 5 μM staurosporine for 4.5 h before MitoTracker labeling (*c*) and double-staining with DAPI (*a*) and affinity-purified R280 antibodies (*b*). (*a*) DAPI staining of nuclei. Arrowheads denote fragmented, condensed nuclei typical of apoptotic cells; the arrow marks a normal, nonapoptotic nucleus. (*b*) R280 staining of pro-caspase-3. Caspase-3 precursor stains in normal cells (*arrow*) but is absent in apoptotic cells (*arrowhead*). (*c*) MitoTracker staining of mitochondria. Mitochondria are labeled with MitoTracker in cells with a normal nucleus (*arrow*) but do not label in cells with apoptotic nuclei (*arrowhead*). (*a–c*) These results are representative of three separate experiments. Bar, 10 μm.

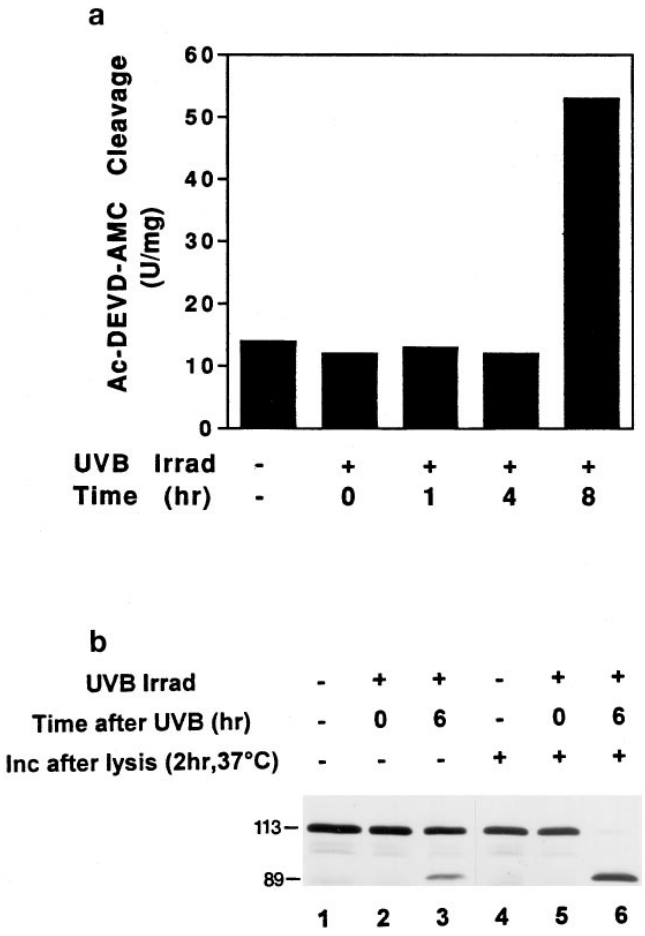

Figure 7. Time course of appearance of cleavage activity in keratinocyte lysates after UVB irradiation. (*a*) Whole cell lysates prepared at various times after UVB irradiation were assayed for cleavage of the fluorogenic substrate Ac-DEVD-AMC as described in the Materials and Methods section. Cleavage activity is expressed in U/mg, where a unit is defined as the amount of enzyme needed to produce 1 pmol per min using 100 μM Ac-DEVD-AMC. Four separate experiments yielded similar results. (*b*) PARP cleavage is observed in keratinocytes 6 h after UV irradiation. Irradiated and control nonirradiated keratinocytes were lysed at the indicated times as described in Materials and Methods. Whole cell lysates (lanes *1–3*), as well as whole cell lysates incubated in vitro for 2 h at 37°C (lanes *4–6*), were immunoblotted with a serum recognizing PARP (Casciola-Rosen et al., 1995). The migration positions of intact PARP (113 kD) and its cleavage fragment (89 kD) are marked. 60 μg of protein was loaded in each lane. This experiment was repeated on three separate occasions with similar results. Identical results were obtained using HeLa cells.

tosolic caspase-3 precursors are equivalent in terms of activation mechanism remains a high priority.

Mitochondrial Caspase-3 Precursor Staining Is Absent in Apoptotic Cells

Our studies demonstrate that the caspase-3 precursor localizes to mitochondria in healthy cells but is absent from this site in apoptotic cells. This loss of caspase-3 precursor staining in mitochondria is induced in a variety of cell types by diverse apoptotic stimuli including UV irradiation, staurosporine, or C2-ceramide. Caspase-3 activity is only detectable in cell populations containing morphologically apoptotic cells, indicating that the loss of mitochondrial caspase-3 staining and caspase-3 activation are temporally linked. The inability of R280 to recognize the mature form of caspase-3, as well as the asynchronous nature of apoptosis in cell populations, prevents us from distinguishing whether caspase-3 activation occurs in mitochondria, or whether the caspase-3 precursor and cytochrome *c* are redistributed from mitochondria before activation.

Interestingly, the mitochondrial pool of caspase-3 colocalizes with cytochrome *c*, which has also been shown to leak from mitochondria into the cytosol early during apoptosis (before alteration of mitochondrial transmembrane potential). Accumulating evidence suggests that the release of cytochrome *c* from mitochondria plays a critical role in initiating the apoptotic process: (*a*) The anti-apoptotic proteins Bcl-2 or Bcl-X_L (which localize to the outer mitochondrial membrane) prevent cytochrome *c* release from mitochondria in vitro and in vivo and prevent activation of caspase-3 (Kluck et al., 1997; Vander Heiden et al., 1997; Yang et al., 1997). (*b*) Cytochrome *c*, in conjunction with two protein cofactors (Apaf-1 and caspase-9/Apaf-3) and dATP/ATP, stimulate the conversion of the caspase-3 precursor to its active form in cell-free systems (Li et al., 1997; Zou et al., 1997). These studies strongly support the hypothesis that spatial separation of interacting proteins is key to modulation of the apoptotic process. This hypothesis predicts that cofactors that participate in cytochrome *c*–mediated processing of caspase-3 (e.g., Apaf-1 and caspase-9) are segregated from the caspase-3 precursor and cytochrome *c* in healthy cells, and that proapoptotic signals permit the efficient formation of an activation complex, with ensuing apoptosis.

The release of cytochrome *c* from mitochondria during apoptosis precedes mitochondrial membrane depolarization (Kluck et al., 1997; Yang et al., 1997), whereas release of AIF requires permeability transition (Susin et al., 1996). These differences might reflect the existence of multiple mechanisms through which mitochondria can influence cell death pathways. The observations that mitochondria in keratinocytes in which apoptosis is induced by UV irradiation still label with MitoTracker but fail to label when apoptosis is induced by staurosporine suggest that these different pathways might be operating to different extents in these settings. Whether active caspase-3 can affect mitochondrial membrane potential remains unknown but is of significant interest.

In conclusion, the coenrichment of caspase-3 at a site containing several molecules that regulate its activation suggests a mechanism whereby the apoptotic stimulus emanating from mitochondria is efficiently transduced. While all apoptotic stimuli appear to converge on a common set of "executioner" proteases, the upstream mechanisms that activate this final common pathway appear to vary for different stimuli. We propose that the mitochondrial subpopulation of caspase-3 precursor molecules is spatially and biochemically distinct and is coupled to a unique subset of apoptotic signaling pathways, which are Bcl-2 sensitive. These apoptotic signals are transduced by bringing together locally enriched but spatially separated molecules

(e.g., cytochrome *c*, caspase-3 precursor, Apaf-1, caspase-9), thus permitting the formation of a multiprotein complex that catalyzes efficient activation of caspase-3. Alternatively, the mitochondrial caspase-3 precursor may have a unique upstream function in some forms of apoptosis, perhaps becoming activated in mitochondria before alteration of mitochondrial physiology. Determining the effects of Bcl-2 family members on the function of this mitochondrial caspase-3 pool is a major priority.

We thank Ann Hubbard for helpful discussions, Greg Martin for assistance with immuno-EM, and Chip Montrose (all three from Johns Hopkins University) for assistance with confocal microscopy.

This work was supported by National Institutes of Health grants 5T32-AI07247 and K12DK01298, a Career Development Award form the Dermatology Foundation/Lever Brothers Co. (LCR), AR44684 (LCR), the Peggy Meyerhoff-Pearlstone Foundation, the Howard Bank Memorial Fund, and an Arthritis Foundation (Maryland Chapter) Institutional Grant. A. Rosen is a Pew Scholar in the Biomedical Sciences.

Received for publication 18 September 1997 and in revised form 22 January 1998.

References

Alnemri, E.S., D.J. Livingston, D.W. Nicholson, G. Salvesen, N.A. Thornberry, W.W. Wong, and J.Y. Yuan. 1996. Human ICE/CED-3 protease nomenclature. *Cell.* 87:171.

Balch, W.E., and J.E. Rothman. 1985. Characterization of protein transport between successive compartments of the Golgi: asymmetric properties of donor and acceptor activities in a cell-free system. *Arch. Biochem. Biophys.* 240:413–425.

Berryman, M.A., W.R. Porter, R.D. Rodewald, and A.L. Hubbard. 1992. Effects of tannic acid on antigenicity and membrane contrast in ultrastructural immunocytochemistry. *J. Histochem. Cytochem.* 40:845–857.

Boldin, M.P., E.E. Varfolomeev, Z. Pancer, I.L. Mett, J.H. Camonis, and D. Wallach. 1995. A novel protein that interacts with the death domain of Fas/APO-1 contains a sequence motif related to the death domain. *J. Biol. Chem.* 270:7795–7798.

Boldin, M.P., T.M. Goncharov, Y.V. Goltsev, and D. Wallach. 1996. Involvement of MACH, a novel MORT1/FADD-interacting protease, in Fas/APO-1- and TNF receptor-induced cell death. *Cell.* 85:803–815.

Casciola-Rosen, L.A., G. Anhalt, and A. Rosen. 1994*a*. Autoantigens targeted in systemic lupus erythematosus are clustered in two populations of surface structures on apoptotic keratinocytes. *J. Exp. Med.* 179:1317–1330.

Casciola-Rosen, L.A., D.K. Miller, G.J. Anhalt, and A. Rosen. 1994*b*. Specific cleavage of the 70-kD protein component of the U1 small nuclear ribonucleoprotein is a characteristic biochemical feature of apoptotic cell death. *J. Biol. Chem.* 269:30757–30760.

Casciola-Rosen, L.A., G.J. Anhalt, and A. Rosen. 1995. DNA-dependent protein kinase is one of a subset of autoantigens specifically cleaved early during apoptosis. *J. Exp. Med.* 182:1625–1634.

Casciola-Rosen, L.A., D.W. Nicholson, T. Chong, K.R. Rowan, N.A. Thornberry, D.K. Miller, and A. Rosen. 1996. Apopain/CPP32 cleaves proteins that are essential for cellular repair: a fundamental principle of apoptotic death. *J. Exp. Med.* 183:1957–1964.

Castedo, M., A. Macho, N. Zamzami, T. Hirsch, P. Marchetti, J. Uriel, and G. Kroemer. 1995. Mitochondrial perturbations define lymphocytes undergoing apoptotic depletion in vivo. *Eur. J. Immunol.* 25:3277–3284.

Chinnaiyan, A.M., and V.M. Dixit. 1996. The cell-death machine. *Curr. Biol.* 6:555–562.

Chinnaiyan, A.M., K. O'Rourke, M. Tewari, and V.M. Dixit. 1995. FADD, a novel death domain-containing protein, interacts with the death domain of Fas and initiates apoptosis. *Cell.* 81:505–512.

Chinnaiyan, A.M., W.L. Hanna, K. Orth, H.J. Duan, G.G. Poirier, C.J. Froelich, and V.M. Dixit. 1996*a*. Cytotoxic T-cell-derived granzyme B activates the apoptotic protease ICE-LAP3. *Curr. Biol.* 6:897–899.

Chinnaiyan, A.M., K. Orth, K. O'Rourke, H.J. Duan, G.G. Poirier, and V.M. Dixit. 1996*b*. Molecular ordering of the cell death pathway: Bcl-2 and Bcl-xL function upstream of the Ced-3-like apoptotic proteases. *J. Biol. Chem.* 271: 4573–4576.

Chinnaiyan, A.M., K. O'Rourke, B.R. Lane, and V.M. Dixit. 1997. Interaction of CED-4 with CED-3 and CED-9: a molecular framework for cell death. *Science.* 275:1122–1126.

Cossarizza, A., C. Franceschi, D. Monti, S. Salvioli, E. Bellesia, R. Rivabene, L. Biondo, G. Rainaldi, A. Tinari, and W. Malorni. 1995. Protective effect of *N*-acetyl-cysteine in tumor necrosis factor-α-induced apoptosis in U937 cells: the role of mitochondria. *Exp. Cell Res.* 220:232–240.

Darmon, A.J., D.W. Nicholson, and R.C. Bleackley. 1995. Activation of the apoptotic protease CPP32 by cytotoxic T-cell-derived granzyme B. *Nature.* 377:446–448.

Deckwerth, T.L., and E.M. Johnson. 1993. Temporal analysis of events associated with programmed cell death (apoptosis) of sympathetic neurons deprived of nerve growth factor. *J. Cell Biol.* 123:1207–1222.

Duan, H., K. Orth, A.M. Chinnaiyan, G.G. Poirier, C.J. Froelich, W.-W. He, and V.M. Dixit. 1996. ICE-LAP6, a novel member of the ICE/Ced-3 gene family, is activated by the cytotoxic T cell protease granzyme B. *J. Biol. Chem.* 271:16720–16724.

Erhardt, P., and G.M. Cooper. 1996. Activation of the CPP32 apoptotic protease by distinct signaling pathways with differential sensitivity to Bcl-x_L. *J. Biol. Chem.* 271:17601–17604.

Gu, Y., C. Sarnecki, M.A. Fleming, J.A. Lippke, R.C. Bleakley, and M.S.S. Su. 1996. Processing and activation of CMH-1 by granzyme B. *J. Biol. Chem.* 271:10816–10820.

Haimowitz-Friedman, A., C.-C. Kan, D. Ehleiter, R.S. Persaud, M. McLoughlin, Z. Fuks, and R.N. Kolesnick. 1994. Ionizing radiation acts on cellular membranes to generate ceramide and initiate apoptosis. *J. Exp. Med.* 180: 525–535.

Hanna, W.L., X. Zhang, J. Turbov, U. Winkler, D. Hudig, and C.J. Froelich. 1993. Rapid purification of cationic granule proteases: application to human granzymes. *Prot. Expr. Purif.* 3:398–404.

Henkart, P.A., and S. Grinstein. 1996. Apoptosis: mitochondria resurrected? *J. Exp. Med.* 183:1293–1295.

Ihrke, G., E.B. Neufeld, T. Meads, M.R. Shanks, D. Cassio, M. Laurent, T.A. Schroer, R.E. Pagano, and A.L. Hubbard. 1993. WIF-B cells: an in vitro model for studies of hepatocyte polarity. *J. Cell Biol.* 123:1761–1775.

Jacobson, M.D., M. Weil, and M.C. Raff. 1996. Role of Ced3/ICE-family proteases in staurosporine-induced programmed cell death. *J. Cell Biol.* 133: 1041–1051.

Jacobson, M.D., M. Weil, and M.C. Raff. 1997. Programmed cell death in animal development. *Cell.* 88:347–354.

Kluck, R.M., E. Bossy-Wetzel, D.R. Green, and D.D. Newmeyer. 1997. The release of cytochrome c from mitochondria: a primary site for Bcl-2 regulation of apoptosis. *Science.* 275:1132–1136.

Krajewski, S., S. Tanaka, S. Takayama, M.J. Schibler, W. Fenton, and J.C. Reed. 1993. Investigation of the subcellular distribution of the Bcl-2 oncoprotein: residence in the nuclear envelope, endoplasmic reticulum, and outer mitochondrial membranes. *Cancer Res.* 53:4701–4714.

Kroemer, G., N. Zamzami, and S.A. Susin. 1997. Mitochondrial control of apoptosis. *Immunol. Today.* 44:44–51.

Li, P., D. Nijhawan, I. Budihardjo, S.M. Srinivasula, M. Ahmad, E.S. Alnemri, and X. Wang. 1997. Cytochrome c and dATP-dependent formation of Apaf-1/caspase-9 complex initiates an apoptotic protease cascade. *Cell.* 91:479–489.

Liu, X., C.N. Kim, J. Yang, R. Jemmerson, and X. Wang. 1996. Induction of apoptotic program in cell-free extracts: requirement for dATP and cytochrome *c*. *Cell.* 86:147–157.

Macho, A., M. Castedo, P. Marchetti, J.J. Aguilar, D. Decaudin, N. Zamzami, P.M. Girard, J. Uriel, and G. Kroemer. 1995. Mitochondrial dysfunctions in circulating T lymphocytes from human immunodeficiency virus-1 carriers. *Blood.* 86:2481–2487.

Martin, S., G. Amarante-Mendes, L. Shi, T.-H. Chuang, C. Casiano, G. O'Brian, P. Fitzgerald, E. Tan, G. Bokoch, A. Greenberg, and D. Green. 1996. The cytotoxic cell protease granzyme B initiates apoptosis in a cell-free system by proteolytic processing and activation of the ICE/CED-3 family protease, CPP32, via a novel two-step mechanism. *EMBO (Eur. Mol. Biol. Organ.) J.* 15:2407–2416.

Martin, S.J., and D.R. Green. 1995. Protease activation during apoptosis: death by a thousand cuts? *Cell.* 82:349–352.

Muzio, M., A.M. Chinnaiyan, F.C. Kischkel, K. O'Rourke, A. Shevchenko, J. Ni, C. Scaffidi, J.D. Bretz, M. Zhang, R. Gentz, et al. 1996. FLICE, a novel FADD-homologous ICE/CED-3-like protease, is recruited to the CD95 (Fas/APO-1) death-inducing signaling complex. *Cell.* 85:817–827.

Muzio, M., G.S. Salvesen, and V.M. Dixit. 1997. FLICE induced apoptosis in a cell-free system—cleavage of caspase zymogens. *J. Biol. Chem.* 272:2952–2956.

Newmeyer, D.D., D.M. Farschon, and J.C. Reed. 1994. Cell-free apoptosis in Xenopus egg extracts: inhibition by Bcl-2 and requirement for an organelle fraction enriched in mitochondria. *Cell.* 79:353–364.

Nicholson, D.W., A. Ali, N.A. Thornberry, J.P. Vaillancourt, C.K. Ding, M. Gallant, Y. Gareau, P.R. Griffin, M. Labele, Y.A. Lazebnik, et al. 1995. Identification and inhibition of the ICE/CED-3 protease necessary for mammalian apoptosis. *Nature.* 376:37–43.

Nicholson, D.W., and W.C. McMurray. 1984. CDP-diglyceride hydrolase from pig liver mitochondria. *Can. J. Biochem. Cell Biol.* 62:1205–1216.

Nicholson, D.W., and N.A. Thornberry. 1997. Caspases: killer proteases. *Trends Biochem. Sci.* 22:299–306.

Nicholson, D.W., H. Kohler, and W. Neupert. 1987. Import of cytochrome c into mitochondria. Cytochrome c heme lyase. *Eur. J. Biochem.* 164:147–157.

Olmsted, J.B. 1981. Affinity purification of antibodies from diazotized paper blots of heterogeneous protein samples. *J. Biol. Chem.* 256:11955–11957.

Orth, K., K. O'Rourke, G.S. Salvesen, and V.M. Dixit. 1996. Molecular ordering of apoptotic mammalian CED-3/ICE-like proteases. *J. Biol. Chem.* 271: 20977–20980.

Petit, P.X., H. Lecoeur, E. Zorn, C. Dauguet, B. Mignotte, and M.-L. Gougeon.

1995. Alterations in mitochondrial structure and function are early events of dexamethasone-induced thymocyte apoptosis. *J. Cell Biol.* 130:157–167.

Quan, L.T., A. Caputo, R.C. Bleakley, D.J. Pickup, and G.S. Salveson. 1995. Granzyme B is inhibited by the cowpox virus serpin cytokine response modifier A. *J. Biol. Chem*. 270:10377–10379.

Quan, L.T., M. Tewari, K. O'Rourke, V. Dixit, S.J. Snipas, G.G. Poirier, C. Ray, D.J. Pickup, and G.S. Salveson. 1996. Proteolytic activation of the cell death protease Yama/CPP32 by granzyme B. *Proc. Natl. Acad. Sci. USA*. 93: 1972–1976.

Reed, J.C. 1994. Bcl-2 and the regulation of programmed cell death. *J. Cell Biol.* 124:1–6.

Reed, J.C. 1997*a*. Cytochrome c: can't live with it—can't live without it. *Cell.* 91: 559–562.

Reed, J.C. 1997*b*. Double identity for proteins of the Bcl-2 family. *Nature.* 387: 773–776.

Rotonda, J., D.W. Nicholson, K.M. Fazil, M. Gallant, Y. Gareau, M. Labele, E.P. Peterson, D.M. Rasper, R. Ruel, J.P. Vaillancourt, et al. 1996. The three-dimensional structure of apopain/CPP32, a key mediator of apoptosis. *Nat. Struct. Biol.* 3:619–625.

Salvesen, G., and V.M. Dixit. 1997. Caspases: intracellular signaling by proteolysis. *Cell.* 91:443–446.

Scoggan, K.A., D.W. Nicholson, and A.W. Ford-Hutchinson. 1996. Regulation of leukotriene-biosynthetic enzymes during differentiation of myelocytic HL-60 cells to eosinophilic or neutrophilic cells. *Eur. J. Biochem.* 230:572–578.

Shi, L., G. Chen, G. MacDonald, L. Bergeron, H. Li, M. Miura, R.J. Rotello, D.K. Miller, T. Seshadri, J. Yuan, and A.H. Greenberg. 1996. Activation of an interleukin 1β converting enzyme-dependent apoptosis pathway by granzyme B. *Proc. Natl. Acad. Sci. USA*. 93:11002–11007.

Strasser, A., A.W. Harris, D.C.S. Huang, P.H. Krammer, and S. Cory. 1995. Bcl-2 and Fas/APO-1 regulate distinct pathways to lymphocyte apoptosis. *EMBO (Eur. Mol. Biol. Organ.) J.* 14:6136–6147.

Susin, S.A., N. Zamzami, M. Castedo, E. Daugas, H.G. Wang, S. Geley, F. Fassy, J.C. Reed, and G. Kroemer. 1997. The central executioner of apoptosis: multiple connections between protease activation and mitochondria in Fas/APO-1/CD95- and ceramide-induced apoptosis. *J. Exp. Med.* 186:25–37.

Susin, S.A., N. Zamzami, M. Castedo, T. Hirsch, P. Marchetti, A. Macho, E. Daugas, M. Geuskens, and G. Kroemer. 1996. Bcl-2 inhibits the mitochondrial release of an apoptogenic protease. *J. Exp. Med.* 184:1331–1341.

Taylor, I.C.A., S. Roy, P. Yaswen, M.R. Stampfer, and H.E. Varmus. 1995. Mouse mammary tumors express elevated levels of RNA encoding the murine homolog of SKY, a putative receptor kinase. *J. Biol. Chem.* 270:6872–6880.

Thompson, C.B. 1995. Apoptosis in the pathogenesis and treatment of disease. *Science.* 267:1456–1462.

Thornberry, N.A., T.A. Ranon, E.P. Peterson, D.M. Rasper, T. Timkey, M. Garcia-Calvo, V.M. Houtzager, P.A. Nordstrom, S. Roy, J.P. Vaillancourt, et al. 1997. A combinatorial approach defines specificities of members of the caspase family and granzyme B. Functional relationships established for key mediators of apoptosis. *J. Biol. Chem.* 272:17907–17911.

Vander Heiden, M.G., N.S. Chandel, E.K. Williamson, P.T. Schumacker, and C.B. Thompson. 1997. Bcl-X_L regulates the membrane potential and volume homeostasis of mitochondria. *Cell.* 91:627–637.

Vaux, D.L. 1997. CED-4: the third horseman of apoptosis. *Cell.* 90:389–390.

Vaux, D.L., and A. Strasser. 1996. The molecular biology of apoptosis. *Proc. Natl. Acad. Sci. USA*. 93:2239–2244.

Vayssiere, J.-L., P.X. Petit, Y. Risler, and B. Mignotte. 1994. Commitment to apoptosis is associated with changes in mitochondrial biogenesis and activity in cell lines conditionally immortalized with simian virus 40. *Proc. Natl. Acad. Sci. USA*. 91:11752–11756.

White, E. 1996. Life, death, and the pursuit of apoptosis. *Genes Dev.* 10:1–15.

Wu, D., H.D. Wallen, and G. Nunez. 1997. Interaction and regulation of subcellular localization of CED-4 by CED-9. *Science.* 275:1126–1129.

Yang, J., X. Liu, K. Bhalla, C.N. Kim, A.M. Ibrado, J. Cai, T.-I. Peng, D.P. Jones, X. Wang, X.S. Liu, et al. 1997. Prevention of apoptosis by Bcl-2: release of cytochrome *c* from mitochondria blocked. *Science*. 275:1129–1132.

Yin, X.-M., Z.N. Oltvai, D.J. Veis-Novack, G.P. Linette, and S.J. Korsmeyer. 1994. Bcl-2 gene family and the regulation of programmed cell death. *Cold Spring Harbor Symp. Quant. Biol.* 59:387–394.

Zamzami, N., P. Marchetti, M. Castedo, D. Decaudin, A. Macho, T. Hirsch, S. Susin, P.X. Petit, G.B. Mignotte, and G. Kroemer. 1995*a*. Sequential reduction of mitochondrial transmembrane potential and generation of reactive oxygen species in early programmed cell death. *J. Exp. Med.* 182:367–377.

Zamzami, N., P. Marchetti, M. Castedo, C. Zanin, J.-L. Vayssiere, P.X. Petit, and G. Kroemer. 1995*b*. Reduction in mitochondrial potential constitutes an early irreversible step of programmed lymphocyte death in vivo. *J. Exp. Med.* 181:1661–1672.

Zamzami, N., S.A. Susin, P. Marchetti, T. Hirsch, I. Gomez-Monterrey, M. Castedo, and G. Kroemer. 1996. Mitochondrial control of nuclear apoptosis. *J. Exp. Med.* 183:1533–1544.

Zou, H., W.J. Henzel, X. Liu, A. Lutschg, and X. Wang. 1997. Apaf-1, a human protein homologous to *C. elegans* CED-4, participates in cytochrome *c*-dependent activation of caspase-3. *Cell.* 90:405–413.